How Does Joint Evolution of Consumer Traits Affect Resource Specialization?*

Paula Vasconcelos and Claus Rueffler†

Department of Ecology and Genetics, Animal Ecology, Uppsala University, Norbyvägen 18D, 752 36 Uppsala, Sweden

ABSTRACT: Consumers regularly experience trade-offs in their ability to find, handle, and digest different resources. Evolutionary ecologists recognized the significance of this observation for the evolution and maintenance of biological diversity long ago and continue to elaborate on the conditions under which to expect one or several specialists, generalists, or combinations thereof. Existing theory based on a single evolving trait predicts that specialization requires strong trade-offs such that generalists perform relatively poorly, while weak trade-offs favor a single generalist. Here, we show that this simple dichotomy does not hold true under joint evolution of two or more foraging traits. In this case, the boundary between trade-offs resulting in resource specialists and resource generalists is shifted toward weaker trade-off curvatures. In particular, weak trade-offs can result in evolutionary branching, leading to the evolution of two coexisting resource specialists, while the evolution of a single resource generalist requires particularly weak trade-offs. These findings are explained by performance benefits due to epistatic trait interactions enjoyed by phenotypes that are specialized in more than one trait for the same resource.

Keywords: competition, evolutionary branching, polymorphism, predator-prey model, trade-off.

Introduction

Competition for shared resources is widely accepted as an important driver for evolutionary diversification (Schluter 2000; Doebeli 2011; Nosil 2012; Pfennig and Pfennig 2012). Over the past 20 years, many theoretical studies have investigated the role of resource competition for evolutionary diversification by delimiting the conditions for the existence of so-called evolutionary branching points (e.g., Kisdi and Geritz 1999; Doebeli and Dieckmann 2000; Claessen

and Dieckmann 2002; Doebeli 2002; Schreiber and Tobiason 2003; Egas et al. 2004, 2005; Ma and Levin 2006; Rueffler et al. 2006b; Débarre and Gandon 2011; Zu et al. 2011a). Evolutionary branching points emerge in models for the long-term evolution of quantitative traits in which fitness is derived from an explicit ecological scenario (Metz et al. 1992, 1996; Geritz et al. 1998; Doebeli 2011). Specifically, evolutionary branching points are trait values that are reached through gradual change of a lineage that evolves uphill on a fitness landscape. However, due to selection being both density and frequency dependent, the fitness landscape is dynamic. As the population evolves uphill, this landscape changes such that the population eventually finds itself in a fitness valley. At this point, directional selection turns into disruptive selection, to which the population responds by evolving increased phenotypic variation (Rueffler et al. 2006a), possibly resulting in ecological speciation (Dieckmann and Doebeli 1999; Geritz and Kisdi 2000; Dieckmann et al. 2004; Bolnick 2006; Schneider and Bürger 2006; Doebeli et al. 2007; Pennings et al. 2008; Kopp and Hermisson 2008; Ripa 2009; Rettelbach et al. 2013).

The specifics of the ecological models underlying competition-driven diversification vary greatly in the above-cited studies. Some authors employ variants of the Lotka-Volterra competition model (Dieckmann and Doebeli 1999; Doebeli and Dieckmann 2000; Bolnick 2006; Pennings et al. 2008), others use Levene's (1953) two-patch model (Geritz et al. 1998; Kisdi and Geritz 1999; Geritz and Kisdi 2000; Débarre and Gandon 2011), and yet others use models with explicit resource dynamics (Claessen and Dieckmann 2002; Doebeli 2002; Schreiber and Tobiason 2003; Egas et al. 2005; Ma and Levin 2006; Rueffler et al. 2006b; Zu et al. 2011a). What these models have in common is that competition between phenotypes is mediated by a single quantitative trait and that phenotypes are subject to trade-offs such that increased specialization for one set of resources or habitats can be achieved only at the cost of decreased specialization for the complementary set of resources or habitats. The broad picture that emerges from these studies is

as follows. A single generalist—an intermediate phenotype that has a similar ability to feed on different resources or utilize different habitats—evolves if this generalist can utilize different resources or habitats relatively well, while evolutionary branching resulting in two coexisting specialists occurs if the generalist cannot utilize different resources or habitats well.

The restriction to a single evolving quantitative trait has its origin in the desire of theoreticians to focus on mathematically tractable models and does not reflect biological reality. For instance, feeding efficiency in the medium ground finch (*Geospiza fortis*) for different types of seeds depends on beak length, beak depth, and beak width simultaneously (Hendry et al. 2009). Similarly, benthic and limnetic three-spine sticklebacks (*Gasterosteus* spp.) differ in both the number and the length of their gill rakers as well as in overall body size and shape. These traits jointly affect their feeding efficiency for alternative resources (e.g., Schluter 1993, 1995). However, feeding efficiency also depends on traits that mediate the interaction between consumers and their resources at stages before and after prey items are captured. For instance, evidence exists that sensory differences due to different color vision genes in capuchin monkeys (*Cebus capucinus*) affect the ability to detect either camouflaged or noncamouflaged insects (Melin et al. 2007), and echolocation call frequencies in bats may determine their ability to detect different parts of the arthropod size spectrum (Siemers and Swift 2006; Safi and Siemers 2010). Once a prey item has been successfully detected and captured, traits of the digestive system can affect the efficiency to extract energy from alternative food resources, as has been reported for birds (Afik and Karasov 1995) and fish (Olsson et al. 2007). Similarly, evidence exists that for some phytophagous insects specific adaptations are needed to overcome the chemical defense of different host plants (Rausher 1984; Mackenzie 1996). These observations suggest that investigating the potential for evolutionary branching in models with several jointly evolving traits is important in order to obtain an understanding of this phenomenon under more realistic conditions.

For a particular trait value to be an evolutionary branching point, it has to fulfil two conditions. First, it has to be reachable through gradual change of a lineage that evolves uphill on a fitness landscape. If this property is fulfilled, we refer to the trait value as an "evolutionary attractor." Second, once the majority of the population has evolved toward this trait value, the fitness landscape must have changed such that the population is located in a fitness valley and therefore invadable by mutants of small phenotypic effect. Thus, the question of how an increased number of jointly evolving traits in a mathematical model affects the potential for evolutionary branching can be broken down into

two parts. First, does increasing the number of jointly evolving traits affect whether a particular evolutionary strategy is an attractor of the evolutionary dynamics? Second, does increasing the number of jointly evolving traits affect whether an evolutionarily attracting strategy is invadable by nearby mutants?

Both questions have been addressed in a few studies. Most prominently, Doebeli and Ispolatov (2010) studied a Lotka-Volterra competition model in which both the carrying capacity and the intensity of competition among different genotypes is described by multidimensional Gaussian functions. In this model, the generalist strategy that maximizes the carrying capacity is an attractor of the evolutionary dynamics independent of the dimension of the trait space. The authors then ask how increasing the number of jointly evolving traits affects whether the carrying capacity maximizing strategy can be invaded by nearby mutants. The results suggest that evolutionary branching becomes an ever more likely outcome of evolution as the dimension of the trait space increases. Two follow-up studies support this prediction. First, Débarre et al. (2014) show that the prediction of Doebeli and Ispolatov (2010) holds for Lotka-Volterra competition models with arbitrary symmetric carrying capacity and competition functions as long as the carrying capacity function is unimodal. Second, Svardal et al. (2014) derive a Lotka-Volterra competition model from an underlying Lotka-Volterra consumer-resource model. These authors assume that the efficiency of consumer individuals for the different objects from a resources distribution is determined according to a key-keyhole mechanism whereby both consumers and resources are characterized by multidimensional trait vectors. In these models, increasing the dimension of the trait space and thereby the number of jointly evolving traits facilitates evolutionary branching because it increases the probability that directions in trait space exist in which the attracting generalist strategy is invadable. The reason for this is twofold. First, if for each trait the invadability of the generalist strategy depends on an independent model parameter, then increasing the dimension of the trait space increases the probability that invasion is possible along at least one axis in trait space. Débarre et al. (2014) refer to this as the combinatorial effect of joint evolution. Second, different traits can interact in their effect on intraspecific competition. As a result, the effect of a change in one trait on fitness can depend on whether this change is accompanied by changes in other traits. Consider two traits that are both under stabilizing selection such that for each trait separately the current trait is at a maximum of the fitness landscape. Thus, mutations that change only one of the trait values are disfavored. However, if traits interact in their effect on fitness, it is possible that mutant individuals that carry changes in both traits are favored by selection. As a

result, once traits evolve jointly, potential evolutionary branching points can be invadable in compound directions of the trait space where several traits change in concert. Débarre et al. (2014) refer to this as evolutionary branching due to epistatic trait interactions.

Another set of studies investigates models in which an evolutionary branching point in a one-dimensional trait space is no longer an attractor of the evolutionary dynamics after the introduction of a second trait axis. Instead, a strategy that is both attracting and invadable in a one-dimensional trait space becomes a saddle point of the evolutionary dynamics in the extended two-dimensional trait space and thus is never approached by an evolving population. Bolnick and Doebeli (2003) and Van Dooren et al. (2004) find that if males and females can evolve independent phenotypes, then competition for resources can result in a sexual dimorphism rather than competition-driven speciation. Leimar (2005) develops a conceptual framework to determine whether evolutionary branching resulting in two coexisting genotypes or the evolution of a single genotype capable of producing offspring with two different phenotypes is the more likely outcome of evolution. His results show that spatially heterogeneous selection favors genetic polymorphism while temporally fluctuating selection and local competition between relatives prevent evolutionary branching if a mixed strategy is developmentally feasible. Concerning temporal fluctuations, Svardal et al. (2011) come to a similar conclusion in a model in which a single genotype produces a continuous distribution of phenotypes due to environmental variation. In these studies, evolution along the second trait axis alters the offspring phenotypic variance such that the population phenotypic variance can increase without increased genetic variance.

In summary, existing studies investigating the effect of multivariate evolution on evolutionary branching give an inconclusive picture. On the one side is a set of studies suggesting that evolutionary branching is facilitated in higher-dimensional trait spaces, but the considered models are special because only the invadability of potential branching points is affected by the dimension of the trait space. On the other side is a set of studies with models purposefully build to incorporate an alternative to the emergence of genetic polymorphism as a response to disruptive selection. What is largely missing are studies in which the multidimensional trait space emerges naturally by allowing for the joint evolution of several parameters with a clear interpretation at the level of the individual. One existing study in this spirit is by Ravigné et al. (2009), who consider habitat specialization in a two-patch model. In their study, a quantitative trait determining the degree of adaptation to one patch or the other is jointly evolving with a trait determining habitat selection. They find that the addition of habitat selection as an evolving trait allows for evolutionary branching under conditions where a single habitat generalist would be the evolutionary end point under random habitat choice.

Here, we investigate evolution in a consumer species that feeds on two resources with a type II functional response. The interaction between consumers and resources is then determined by the feeding efficiencies, the handling times, and the conversion efficiencies for the two resources. We assume that each of these traits is subject to a trade-off. For instance, a consumer phenotype with a short handling time for one resource needs more time to handle the alternative resource. And a mutation reducing the handling time for one resource comes at the cost of an increased handling time for the other, with the coupling of the two handling times being determined by a trade-off curve. Previously, Rueffler et al. (2006b) investigated the conditions for evolutionary branching in each of these traits separately and found that evolutionary branching leading to consumer diversification occurs for suitable trade-off curvatures in feeding efficiency but never in handling time or conversion efficiency. Here, we extend this study by allowing the three traits to evolve jointly. Our most important findings are that, by increasing the number of jointly evolving traits, the conditions for the evolution of a single generalist species become more restricted and that the trade-off curvatures resulting in evolutionary branching are shifted from strong trade-offs toward weaker trade-offs. Whether this makes evolutionary branching more or less likely than previously anticipated depends on which trade-off curvatures are more likely to be realized in nature. If diversification occurs, it results in two specialist consumer phenotypes that are specialized in all of their traits for resource 1 and resource 2, respectively.

Model

We consider a population of consumers feeding on two substitutable resources. To describe the dynamics of these species, we use a two-resource version of the Rosenzweig-MacArthur (1963) model:

$$\frac{dR_1}{dt} = r_1 R_1 \left(1 - \frac{R_1}{K_1}\right) - \frac{R_1 e_1 C}{1 + R_1 e_1 h_1 + R_2 e_2 h_2}, \quad (1a)$$

$$\frac{dR_2}{dt} = r_2 R_2 \left(1 - \frac{R_2}{K_2}\right) - \frac{R_2 e_2 C}{1 + R_1 e_1 h_1 + R_2 e_2 h_2}, \quad (1b)$$

$$\frac{dC}{dt} = C\left(\frac{\alpha_1 R_1 e_1 + \alpha_2 R_2 e_2}{1 + R_1 e_1 h_1 + R_2 e_2 h_2} - d\right), \quad (1c)$$

where C denotes the density of the consumer species and R_1 and R_2 denote the densities of the two resources. In the absence of consumers, resources grow logistically with intrinsic growth rate r_i and carrying capacity K_i. Thus, the

resources do not compete with one another. Consumers forage according to a type II functional response with resource-specific feeding efficiencies e_i and handling times h_i. They have a linear numerical response and convert resources with efficiency α_i into consumer biomass. Finally, d gives the per capita death rate of the consumer. This population dynamical model can exhibit predator-prey cycles, but here we restrict the analysis to parameter combinations for which the system reaches its unique internal fixed-point equilibrium, denoted $\hat{R}_1$, $\hat{R}_2$, and $\hat{C}$ (see app. A for full expressions; apps. A–E are available online).

We assume that the consumer species can evolve in its feeding efficiencies e_i, handling times h_i, and conversion efficiencies α_i. The empirical literature documents that the extent to which consumers can improve on two resources simultaneously is constrained (e.g., Schluter 1993, 1995; Benkman 1993). So once consumers reach this constraint, an improvement in the performance for one resource can only be attained by a reduction in performance for the other (Levins 1962). We implement this constraint as a trade-off curve in the space of performances x_1 and x_2, where x stands for α, e, or h, as shown in figure 1, and restrict the evolutionary dynamics to these trade-off curves. Specifically, we parametrize the values $x = (x_1, x_2)$ that constitute the trade-off curve in a parameter θ_x varying between 0 and 1 and consider θ_x the evolving trait. The parametrization of the trade-off curves is such that $\theta_x = 0$ corresponds to a specialist for resource 1, $\theta_x = 1$ corresponds to a specialist for resource 2, and $\theta_x = 0.5$ corresponds to the generalist that is equally specialized for both resources. Note that a consumer species specialized for resource i is characterized by high values of the feeding efficiency e_i and the conversion efficiency α_i but by low values for the handling time h_i. Thus, the trade-off curves for the different traits require different formulas. Following Nurmi and Parvinen (2013), we use

$$\boldsymbol{x}(\theta_x) = \left(x_{1\,\mathrm{max}} \frac{1 - e^{-z_x(1-\theta_x)}}{1 - e^{-z_x}}, x_{2\,\mathrm{max}} \frac{1 - e^{-z_x\theta_x}}{1 - e^{-z_x}} \right) \quad (2)$$

to parametrize the trade-off in α and e and

$$\boldsymbol{x}(\theta_x) =$$

$$\left(x_{1\,\mathrm{max}} - x_{1\,\mathrm{min}} \frac{1 - e^{-z_x(1-\theta_x)}}{1 - e^{-z_x}}, x_{2\,\mathrm{max}} - x_{2\,\mathrm{min}} \frac{1 - e^{-z_x\theta_x}}{1 - e^{-z_x}} \right) \quad (3)$$

to parametrize the trade-off in h. Here, $x_{1\mathrm{max}}$, $x_{2\mathrm{max}}$, $x_{1\mathrm{min}}$, and $x_{2\mathrm{min}}$ are positive constants determining the range of values the traits can take. The parameter z_x determines the curvature of the trade-off curve; $z_x < 0$ corresponds to trade-off curves for which the generalist does not perform well (convex curves for α and e and concave curves for h), whereas $z_x > 0$ corresponds to trade-off curves for which the generalist does perform well (concave curves for α and e and convex curves for h; see fig. 1). Therefore, we refer to trade-offs with $z_x < 0$ as strong and trade-offs with $z_x > 0$ as weak.
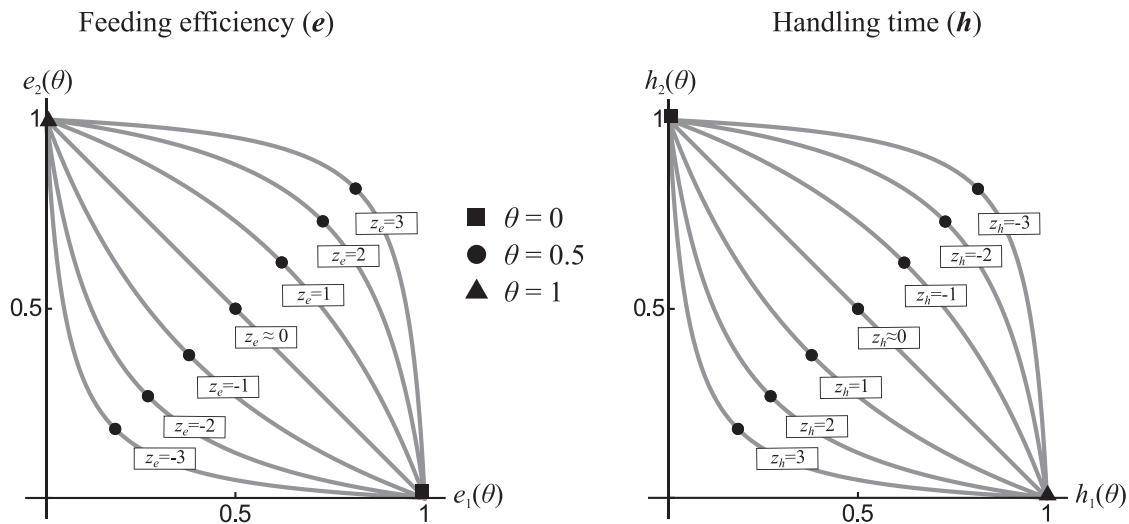
Feeding efficiency (*e*)   Handling time (*h*)

Figure 1: Trade-off curves for feeding efficiency $\boldsymbol{e}$ (*left*) and handling time $\boldsymbol{h}$ (*right*) as determined by equations (2) and (3), respectively. The trade-off curves are parametrized such that $\theta_x = 0$ corresponds to a specialist for resource 1 (black square), $\theta_x = 1$ corresponds to a specialist for resource 2 (black triangle), and $\theta_x = 0.5$ corresponds to the generalist (black circle). Note that this requires that the trade-off curves are parametrized in opposite directions for $\boldsymbol{e}$ and $\boldsymbol{h}$. Furthermore, the values z_e and z_h determine the curvature (strength) of the trade-offs such that positive values result in weak trade-offs and negative values result in strong trade-offs (see text for detailed explanations). In this figure and throughout this study, $e_{1\,\mathrm{max}} = 1 = e_{2\,\mathrm{max}}$, $h_{1\,\mathrm{max}} = 1 = h_{2\,\mathrm{max}}$, and $h_{1\,\mathrm{min}} = 1 = h_{2\,\mathrm{min}}$.

Note that equations (2) and (3) are not defined for $z_x = 0$. But since

$$\lim_{z_x \to 0} x(\theta_x) = (x_{1\max}(1 - \theta_x), x_{2\max}\theta_x) \quad \text{for } x \in \{e, \alpha\}$$

and

$$\lim_{z_x \to 0} x(\theta_x) =$$
$$(x_{1\max} - x_{1\min}(1 - \theta_x), x_{2\max} - x_{2\min}\theta_x) \quad \text{for } x = h,$$

it is natural to define $x(\theta_x)$ according to these limits when $z_x = 0$ (Nurmi and Parvinen 2013). This linear trade-off separates strong from weak trade-offs.

To investigate evolution, we use the adaptive dynamics approximation, which applies to large populations and is based on the technical assumption of rare mutations of small effect (Metz et al. 1992, 1996; Dieckmann and Law 1996; Geritz et al. 1998). We denote the resident's trait values by θ_α^r, θ_e^r, and θ_h^r and the mutant's trait values by θ_α^m, θ_e^m, and θ_h^m. We collect these trait values in the vectors θ^r and θ^m. Assuming that mutations affecting θ are rare allows for the separation of ecological and evolutionary timescales. Thus, the resident population reaches its population dynamical equilibrium before a new mutant appears. This assumption is made for technical reasons, but many individual-based simulations show that the conclusions are robust to violations of the strict timescale separation (e.g., Dieckmann and Doebeli 1999; Kisdi and Geritz 1999; Champagnat et al. 2006; van Doorn et al. 2009; Svardal et al. 2011, 2014). The initial fate of a mutant is determined by its invasion fitness

$$w(\theta^m, \theta^r) = \frac{\alpha_1(\theta_\alpha^m)\hat{R}_1(\theta^r)e_1(\theta_e^m) + \alpha_2(\theta_\alpha^m)\hat{R}_2(\theta^r)e_2(\theta_e^m)}{1 + \hat{R}_1(\theta^r)e_1(\theta_e^m)h_1(\theta_h^m) + \hat{R}_2(\theta^r)e_2(\theta_e^m)h_2(\theta_h^m)} - d,$$

$$(4)$$

which describes its expected per capita growth rate while rare in a resident population at equilibrium (Metz et al. 1992; Metz 2008). Invasion fitness is a function not only of the mutant's trait values but also of the resident's. This is because the resource equilibrium densities $\hat{R}_1$ and $\hat{R}_2$ are determined by the trait values of the resident consumer. If $w(\theta^m, \theta^r) > 0$, the mutant has a positive probability to invade the resident population, but if $w(\theta^m, \theta^r) < 0$, the mutant surely becomes extinct. For $\theta^m = \theta^r$, mutant and resident are indistinguishable, and since the resident population is at equilibrium where it neither grows nor shrinks, we have that $w(\theta^m, \theta^r) = 0$.

The fitness gradient $S(\theta^r)$ with entries

$$S_x(\theta^r) = \left.\frac{\partial w(\theta^m, \theta^r)}{\partial \theta_x^m}\right|_{\theta^m = \theta^r} \quad (5)$$

gives the direction in which fitness increases fastest in multivariate trait space. If $S(\theta^r) \neq 0$ and mutational effects are sufficiently small, then invasion of θ^m implies extinction of

θ^r (see app. B in Dercole and Rinaldi 2008), resulting in a trait substitution sequence. The evolutionary trajectory in the limit of rare mutations of infinitesimal small increments in a very large population—such that drift can be ignored—can be approximated by

$$\frac{d\theta^r}{dt} = c(\theta^r)M(\theta^r)S(\theta^r), \quad (6)$$

where $c(\theta^r)$ is a real-valued function describing variation in the rate of mutations in the resident (e.g., due to variation in population size) and M is the mutational variance-covariance matrix describing a symmetric distribution of mutations around the resident strategy θ^r (Dieckmann and Law 1996; Durinx et al. 2008). A gradient equation for the evolutionary dynamics akin to equation (6) can also be derived from the quantitative genetics approximation in which all genotypes are present at the same time. Then, θ^r characterizes the mean phenotype, the variance-covariance matrix describes the distribution of the standing genetic variation, and the factor $c(\theta^r)$ is a constant (Lande 1979; Abrams et al. 1993; Débarre et al. 2014).

Directional selection vanishes at trait vectors where $S(\theta^r) = 0$. These are known as "singular points" (Geritz et al. 1998), and we denote them by θ^*. Singular points can be either attractors or repellers of the evolutionary dynamics described by equation (6). In addition, a resident population with trait vector θ^* can be either invadable or uninvadable by nearby mutants. In one-dimensional trait spaces—when only one of the traits θ_α, θ_e, or θ_h evolves—these two properties allow for a complete classification (Geritz et al. 1998). Singular points that are attracting and uninvadable are "evolutionary traps" such that no further evolution is possible through small mutations. Singular points that are attracting and invadable are known as evolutionary branching points. At such points, successful nearby mutants do not replace the individuals with the singular trait value, but they can coexist with them. Further selection results in increased divergence between the two trait lineages. If a singular point is repelling, though, the evolutionary dynamics leads away from it regardless of whether it is invadable or uninvadable.

The situation is more complicated if at least two of the traits θ_α, θ_e, and θ_h evolve jointly. In this case, whether or not a singular trait vector θ^* is an attractor of the evolutionary dynamics described by equation (6) depends both on the fitness gradient $S(\theta^r)$ in the neighborhood of the singular point θ^* and on the mutational variance-covariance matrix M that governs the magnitude and direction of mutations. In the following, we briefly describe the mathematical conditions for attractivity and invadability in multidimensional trait spaces. This presentation closely follows Leimar (2009; see also Doebeli 2011).

Invadability of a singular point $\boldsymbol{\theta}^*$ by nearby mutants is determined by the selection Hessian H with entries

$$h_{xy} = \left.\frac{\partial^2 w(\boldsymbol{\theta}^{\mathrm{m}}, \boldsymbol{\theta}^{\mathrm{r}})}{\partial \theta_x^{\mathrm{m}} \partial \theta_y^{\mathrm{m}}}\right|_{\boldsymbol{\theta}^{\mathrm{m}}=\boldsymbol{\theta}^{\mathrm{r}}=\boldsymbol{\theta}^*}, \tag{7}$$

where $x, y \in \{\alpha, e, h\}$. Note that since this matrix of second-order partial derivatives is symmetric, all of its eigenvalues are real. A resident population with the singular strategy $\boldsymbol{\theta}^*$ is uninvadable if it is at a maximum of the fitness landscape resulting from the resource equilibrium densities determined by the resident population itself. This is the case when all eigenvalues of H are negative (H is negative definite). If the Hessian has both positive and negative eigenvalues (H is indefinite), then the singular point is invadable by some nearby mutants but not by others. It is then a saddle point of the fitness landscape (fig. 2b). Finally, if all

eigenvalues of H are positive (H is positive definite), then the singular point can be invaded by all nearby mutants.

Whether or not a singular point $\boldsymbol{\theta}^*$ is an attractor of the evolutionary dynamics described by equation (6) can be determined by a linear stability analysis around $\boldsymbol{\theta}^*$. From this follows that attractivity of $\boldsymbol{\theta}^*$ is determined by the eigenvalues of the matrix MJ. Here, J is the Jacobian of the selection gradient with entries

$$j_{xy} = h_{xy} + q_{xy}, \tag{8}$$

where

$$q_{xy} = \left.\frac{\partial^2 w(\boldsymbol{\theta}^{\mathrm{m}}, \boldsymbol{\theta}^{\mathrm{r}})}{\partial \theta_x^{\mathrm{m}} \partial \theta_y^{\mathrm{r}}}\right|_{\boldsymbol{\theta}^{\mathrm{m}}=\boldsymbol{\theta}^{\mathrm{r}}=\boldsymbol{\theta}^*} \tag{9}$$

are mixed partial derivatives with respect to both mutant and resident traits. The singular point $\boldsymbol{\theta}^*$ is an attractor of
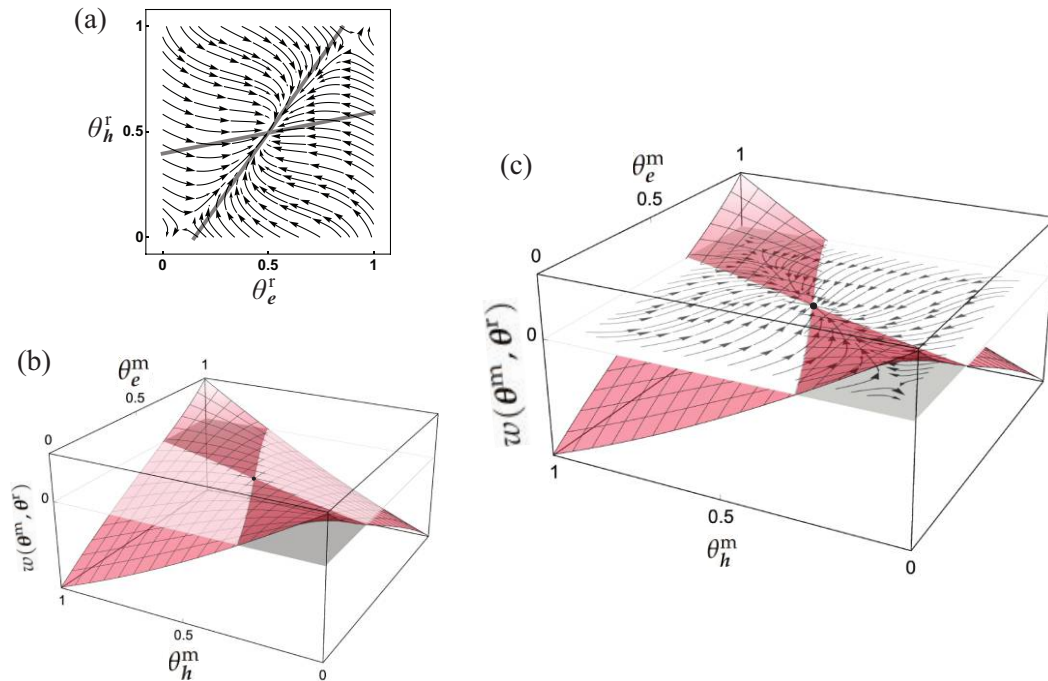

Figure 2: Characterization of the singular point $\boldsymbol{\theta}_{e,h}^* = (0.5, 0.5)$ in terms of attractivity and invadability. *a*, Phase-plane diagram of the joint evolutionary dynamics of the two traits θ_e and θ_h as defined by equation (6) with M equal to the identity matrix. Arrows indicate evolutionary trajectories for different initial conditions. Next to the symmetric singular point $\boldsymbol{\theta}_{e,h}^* = (0.5, 0.5)$ two further singular points exist at $\boldsymbol{\theta}_{e,h}^* \approx (0.11, 0.09)$ and $\boldsymbol{\theta}_{e,h}^* \approx (0.89, 0.91)$. The singular point $\boldsymbol{\theta}_{e,h}^* = (0.5, 0.5)$ is an attractor of the evolutionary dynamics for all initial populations except for those that are highly specialized in both traits for the same resource. Both eigenvalues of the matrix MJ evaluated at $\boldsymbol{\theta}_{e,h}^* = (0.5, 0.5)$ are negative, and the gray lines show the directions of the corresponding eigenvectors. The two flanking singular points are saddle points that are attracting from some directions and repelling into others. *b*, The red surface gives invasion fitness $w(\boldsymbol{\theta}^{\mathrm{m}}, \boldsymbol{\theta}^{\mathrm{r}})$ at the singular point $\boldsymbol{\theta}^{\mathrm{r}} = \boldsymbol{\theta}_{e,h}^* = (0.5, 0.5)$ for values of θ_h^{m} and θ_e^{m} as given by the *X*- and *Y*-axes, respectively. When the mutant strategy equals the resident strategy, $\boldsymbol{\theta}^{\mathrm{r}} = (0.5, 0.5) = \boldsymbol{\theta}^{\mathrm{m}}$, then $w(\boldsymbol{\theta}^{\mathrm{m}}, \boldsymbol{\theta}^{\mathrm{r}}) = 0$ (black circle). Mutants $\boldsymbol{\theta}^{\mathrm{m}}$ have the potential to invade if $w(\boldsymbol{\theta}^{\mathrm{m}}, \boldsymbol{\theta}_{e,h}^*) > 0$ (the fitness landscape is above the transparent plane) and surely become extinct if $w(\boldsymbol{\theta}^{\mathrm{m}}, \boldsymbol{\theta}_{e,h}^*) < 0$ (the fitness landscape is below the transparent plane). The first is the case for mutants that are specialized to a similar degree and for the same resource, while the latter is the case for all other mutants. Thus, the Hessian matrix H has one positive and one negative eigenvalue. *c* combines the information from *a* and *b*. To determine the set of mutants that are able to invade it is sufficient to view the contour plot of the fitness landscape that indicates whether invasion fitness is positive (shaded area on the phase plane) or negative (unshaded area). This is the information given in figure 5b–5h. Parameter values are as in figure 5e.

the evolutionary dynamics if all eigenvalues of the matrix MJ have negative real parts and a repeller if at least one eigenvalue has a positive real part.

Leimar (2009) shows that if the symmetric part of J, defined as $J_{sym} = (J + J^T)/2$, is negative definite (all eigenvalues negative), then the singular point θ^* is an attractor of the evolutionary dynamics described by equation (6) regardless of the mutational variance-covariance matrix M. We refer to this property as "strongly attracting." If J_{sym} is indefinite, then it is possible that the singular point θ^* is an attractor for some M but not for others. We call a singular point "weakly attracting" if it is not strongly attracting, and indeed matrices M exist such that all eigenvalues of MJ have negative real parts. Finally, we call a singular point an "evolutionary repeller" if MJ has at least one eigenvalue with positive real part regardless of the mutational variance-covariance matrix M.

A further complexity for determining evolutionary branching points in multidimensional trait spaces is that attractivity and invadability are necessary but not sufficient conditions. Geritz et al. (2016) describes the full set of conditions and their interconnections. These conditions are (i) attraction, (ii) invadability, (iii) nearby population dynamical coexistence, (iv) nearby disruptive selection, and (v) nearby evolutionary coexistence. The relationship between these conditions is as follows: conditions i and ii are independent, condition iii is implied by conditions i and ii in the strongly attracting case (which includes the case of one-dimensional trait spaces) but in general is independent, conditions ii and iii always imply condition iv, and finally condition iii is necessary for condition v but not sufficient, except when the trait space is one or two dimensional.

Based on the results of Geritz et al. (2016), we classify singular points θ^* as described in figure 3. In short, a singular point θ^* is an end point of the evolutionary dynamics if it is either weakly or strongly attracting and uninvadable (H negative definite). It is an evolutionary branching point if instead H is not negative semidefinite (at least one positive eigenvalue). Where necessary, we then confirm that conditions iii and v are fulfilled. Finally, a singular point θ^* is repelling if it is neither strongly nor weakly attracting such that MJ has at least one eigenvalue with positive real part for any mutational variance-covariance matrix M. For detailed calculations, see appendix C.

With individual-based simulations we investigate to what extent our analytical results are robust to violations of the assumptions of adaptive dynamics. Specifically, these simulations include demographic stochasticity due to finite population size, variable mutational step size, and mutation rates that violate the separation of ecological and evolutionary timescales. For simulation results and methodological details, we refer to appendix D. Simulation code and a Mathematica notebook (Wolfram Research 2019) can be found in the Dryad Digital Repository (https://doi.org/10.5061/dryad.ns1rn8pnf; Vasconcelos and Rueffler 2020).
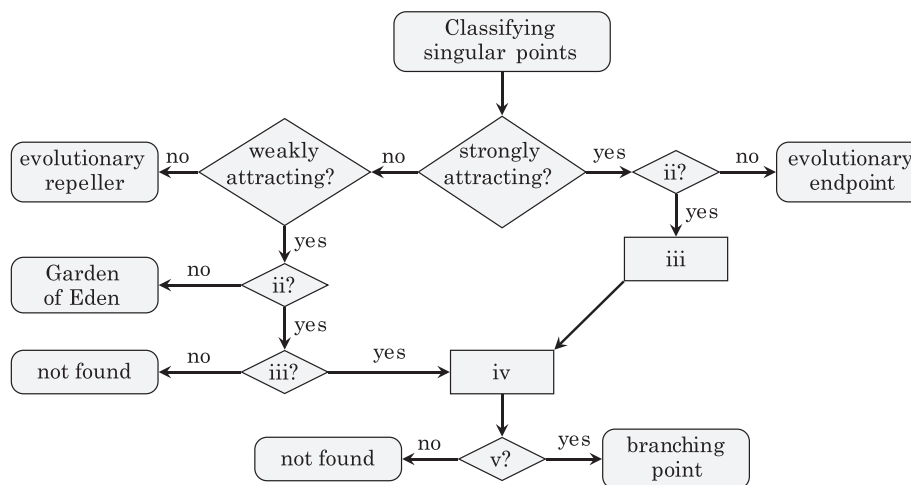

Figure 3: Flow chart for the classification of singular points θ^* in the present model. Roman numbers refer to the following properties of θ^*, as described in Geritz et al. (2016): (ii) invadability, (iii) nearby population dynamical coexistence, (iv) nearby disruptive selection, and (v) nearby evolutionary coexistence. Arrows pointing toward square boxes correspond to implications proven in Geritz et al. (2016). Note that iv implies v for the case of two jointly evolving traits, but this implication needs to be evaluated separately for the case of three jointly evolving traits. A singular point is classified as weakly attracting if it is not strongly attracting, but mutational variance-covariance matrices M exist such that all eigenvalues of the matrix MJ have negative real parts, where J is defined as in equation (8). For matrices M for which MJ has eigenvalues with positive real part, the singular point behaves as an evolutionary repeller.

Results

Evolution of the Three Traits Separately

To contextualize the effect of joint trait evolution, we start by presenting the results for the case that each trait evolves separately while the others remain fixed. These results are qualitatively identical to those described for a very similar model by Rueffler et al. (2006*b*). We investigate three cases: evolution in feeding efficiency e, handling time h, and conversion efficiency α. The results are summarized in figure 4, and the derivation is presented in appendix B. For simplicity, we here focus on the case that the two traits that are not considered evolving are symmetric. For instance, for the case that e is evolving we assume $h_1 = h_2$ and $\alpha_1 = \alpha_2$. Together with the assumptions $r_1 = r_2$ and $K_1 = K_2$, it follows, for symmetry reasons, that the generalist strategy $\theta_x = 0.5$ for $x \in \{\alpha, e, h\}$ is a singular point—that is, the trait value where directional selection vanishes and the fitness landscape is locally flat. Figure E4*a* and figure E4*b* (figs. D1–D4, E1–E6 are available online) show that breaking these symmetry assumptions does not affect the results qualitatively.

For all three traits, the generalist is an attracting and uninvadable singular point for weak trade-offs ($z_x > 0$). For strong trade-offs ($z_x < 0$), the generalist is an evolutionary repeller for both h and α (fig. 4*b*), but for e it changes from an evolutionary branching point to a repeller with increasing strength of the trade-off (fig. 4*a*). In addition, for e the branching point is flanked by two repelling singular points, which collide with the generalist strategy where it loses its attractivity. In this case, the evolutionary end point depends on initial conditions. Populations with initial trait values that are more extreme than those of the flanking repellers evolve to become a specialist for either resource 1 or resource 2, while populations with initial trait values between the flanking repellers evolve toward the generalist strategy and subsequently undergo evolutionary branching.

To understand why the consumer traits differ in their evolutionary dynamics, it is important to understand how they affect resource densities. If the resident population has a higher feeding efficiency for, say, resource 1 than resource 2, then equations (1) show that, everything else being equal, more resource 1 than resource 2 is consumed. As a consequence, in this case resource 1 is less common than resource 2 at equilibrium ($\hat{R}_1 < \hat{R}_2$; app. B, sec. B.1). This gives a benefit to mutants with an increased feeding efficiency for the more abundant resource 2 at the cost of having a lower feeding efficiency for the less common resource 1. Thus, the differential impact of the resident strategy on the resource equilibria gives a rare type of advantage to mutants and selection is negatively frequency dependent. This is a prerequisite for evolutionary branching and coexistence of different consumer genotypes (Heino et al. 1998).

The situation is fundamentally different when the resident consumer is specialized in terms of its handling time for one resource or the other (app. B, sec. B.2). From equations (1) we can see that the two handling times h_1 and h_2 affect the dynamics of the resources in the very same way, namely, through the denominator of the second term on the right-hand side of equations (1a) and (1b). The fraction $1/(1 + R_1 e_1 h_1 + R_2 e_2 h_2)$ can be interpreted as the proportion of time the consumer has available for searching resources instead of handling them (Holling 1959). Thus, changing the handling times changes the consumer's search time, and this affects the two resources equally. As a result, the equilibrium resource densities $\hat{R}_1$ and $\hat{R}_2$ are equal to each other regardless of the degree of specialization of the resident population (app. B, eq. [B9]). A similar argument applies when the resident consumer is specialized in terms of its conversion efficiencies (app. B, sec. B.2). From equations (1), we can see that α_1 and α_2 do not influence the resource dynamics directly but do so only indirectly through the consumer density. Thus, changes in the conversion efficiencies change the consumer density, and this has an equal effect on the two resources. Consequently, the equilibrium resource densities $\hat{R}_1$ and $\hat{R}_2$ are again equal to each other regardless of the degree of specialization of the resident population (app. B, eq. [B15]).

In the case of evolving handling times or evolving conversion efficiencies, the effect of the resident population on the mutant's invasion fitness can be captured in a single variable, namely, $\hat{R}_1 = \hat{R}_2$. Under this condition, one can prove that the trait values θ_α and θ_h that minimize $\hat{R}_i$ are uninvadable attractors of the evolutionary dynamics and that stable coexistence of different strategies is impossible (Metz et al. 2008).

For handling h and conversion efficiency α, the preceding argument implies that the evolutionary dynamics are independent of any specific choice for the functional form of the trade-off curve as long as it is symmetric around the generalist strategy and its curvature does not change sign. For feeding efficiency e, an analysis independent of a specific functional form is possible by using critical function analysis (de Mazancourt and Dieckmann 2004). Such an analysis shows that the bifurcation diagram shown in figure 4*a* is general (Zu et al. 2011*b*).

Jointly Evolving Traits

For jointly evolving traits we find that the evolutionary dynamics depends on the number and combination of evolving traits. To obtain a full understanding, we first describe the evolutionary dynamics for the three different combinations of pairwise evolving traits and afterwards the case of three jointly evolving traits. Results from individual-based
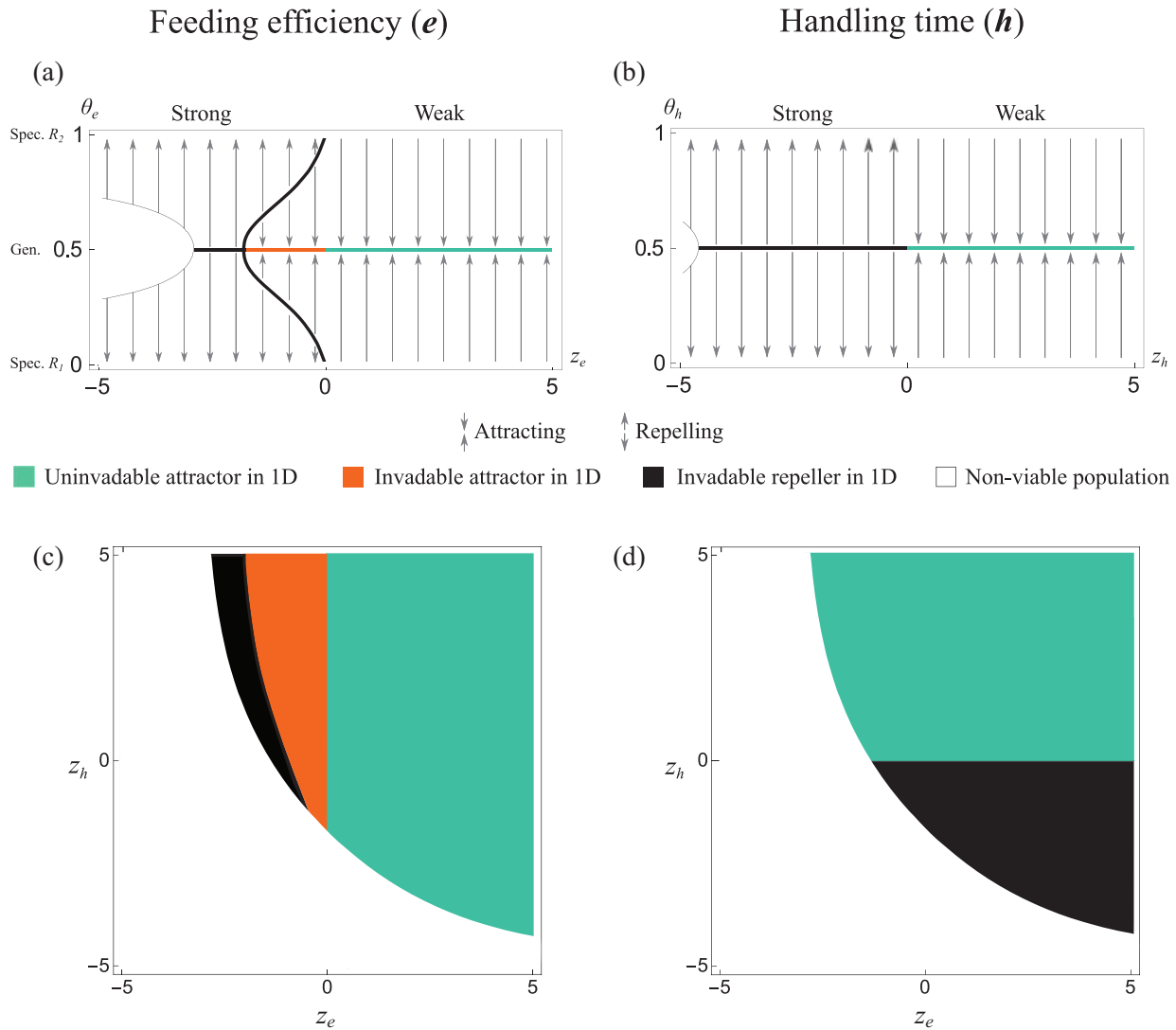
Figure 4: Evolutionary dynamics for feeding efficiency e (a, c) and handling time h (b, d) for symmetric parameter values. The evolutionary dynamics of conversion efficiency α is identical to that of handling time. In a and b, the X-axis gives the curvature parameters z_e and z_h, respectively, and the Y-axis gives the trait space of the evolving traits θ_e and θ_h, respectively. The location of singular points is shown by colored lines. Arrows indicate the direction of the fitness gradient (eq. [5]). a, When feeding efficiency e evolves by itself, the generalist strategy $\theta_e = 0.5$ is invadable for strong trade-offs ($z_e < 0$) and uninvadable for weak trade-offs ($z_e > 0$). It is furthermore attracting for weak and moderately strong trade-offs and repelling for very strong trade-offs. Thus, the generalist strategy is an evolutionary repeller for very strong trade-offs, an evolutionary branching point for moderately strong trade-offs, and an evolutionary end point (uninvadable attractor) for weak trade-offs. Note that the branching point is flanked by two repelling singular points. b, When handling time h evolves by itself, the generalist strategy $\theta_h = 0.5$ is an uninvadable attractor for weak trade-offs and an invadable repeller for strong trade-offs. c, Bifurcation diagram delimiting different evolutionary behaviors at the singular point $\theta_e^* = 0.5$ as a function of the trade-off curvature parameters z_e (X-axis) and different values of the handling times h_1 and h_2. While in a the handling times are fixed at $h_1 = 0 = h_2$, in this plot the handling times are determined according to equation (3) with $h_{1\,max} = 1 = h_{2\,max}$, $h_{1\,min} = 1 = h_{2\,min}$, and $\theta_h = 0.5$ (resulting in symmetric handling times $h_1 = h_2$) and different values of the trade-off curvature parameter z_h (Y-axis). For $z_h = 5$, the trade-off is very weak and $h_1 = h_2$ approach zero as in a. For decreasing values of z_h (increasing values of $h_1 = h_2$), the range of trade-off curvatures resulting in evolutionary branching in e becomes more narrow, and the range of trade-off curvatures resulting in a nonviable population (white region) becomes broader. In d, the analogous information is given for the singular point $\theta_h^* = 0.5$. Here, the values for the feeding efficiencies are determined according to equation (2) with $e_{1\,max} = 1 = e_{2\,max}$, $\theta_e = 0.5$ (resulting in symmetric feeding efficiencies $e_1 = e_2$), and different values of the trade-off curvature parameter z_e (X-axis). For $z_e = 5$, the trade-off is very weak, and $e_1 = e_2$ approach 1, as in b. Comparing these bifurcation diagrams with figure 5a allows us to asses the effect of joint trait evolution. Other parameter values: $K_1 = 2.5 = K_2$, $\alpha_1 = 1 = \alpha_2$, $d = 0.9$, $h_1 = 0 = h_2$ (for a), $e_1 = 1 = e_2$ (for b).

simulations are presented in appendix D and confirm our analytical and numerical findings.

We start by treating joint evolution of *e* and *h* in detail. Joint evolution of *e* and *α* gives very similar results and is therefore treated only briefly. As a third case we treat the joint evolution of *h* and *α*. This case has particularly simple dynamics, as it does not allow for evolutionary branching.

Joint Evolution of Feeding Efficiency and Handling Time. To be able to obtain analytical results, we focus on symmetric parameters $r_1 = r_2$, $K_1 = K_2$, and $\alpha_1 = \alpha_2$. Results for asymmetric parameters are shown in figure E4c. From the symmetry assumptions it follows that the two-dimensional generalist strategy $\theta^*_{e,h} = (\theta^*_e, \theta^*_h) = (0.5, 0.5)$ is a singular point. Figure 5a shows the properties of this singular point as a function of the trade-off curvature parameters z_e and z_h (for results based on alternative parameter values, see fig. E3). This bifurcation diagram should be compared with figure 4c and figure 4d, which show analogous diagrams but for the case that only feeding efficiency *e* or only handling time *h* evolve, respectively. The bifurcation diagrams can be divided into four quadrants, depending on whether both trade-offs are strong, only one of them is strong, or both are weak.

Strong trade-off for e and strong trade-off for h (bottom left quadrant in fig. 5a). The singular point $\theta^*_{e,h}$ is always an invadable repeller (fig. 5b). Evolutionary diversification cannot occur, and evolution leads, depending on initial conditions, to a single phenotype that is either specialized in both traits for resource 1 ($e_1 \gg e_2$ and $h_1 \ll h_2$) or specialized in both traits for resource 2 ($e_1 \ll e_2$ and $h_1 \gg h_2$). Comparing this quadrant with the corresponding quadrant in figure 4c shows that the possibility for evolutionary branching that is present when only feeding efficiency evolves disappears when it evolves jointly with handling time. The reason is that under joint trait evolution, the singular point $\theta^*_{e,h}$ is not attracting anymore.

Weak trade-off for e and strong trade-off for h (bottom right quadrant in fig. 5a). Figure 4c and figure 4d show that in this parameter region θ^*_e is an uninvadable attractor while θ^*_h is an invadable repeller. Based on these results, one might expect that under joint trait evolution the singular point is a saddle point of the evolutionary dynamics that is attracting from some directions and repelling into others, resulting in the evolution of a single specialized phenotype. The analysis of the joint evolutionary dynamics confirms this intuition (fig. 5h) except for a narrow band in which the trade-off for *h* is strong but almost linear. In this latter region, the singular point is weakly attracting, and evolutionary branching is possible for suitable mutational variance-covariance matrices.

Strong trade-off for e and weak trade-off for h (upper left quadrant in fig. 5a). In this parameter region, three different outcomes are possible. For very strong trade-offs in *e*, the singular point $\theta^*_{e,h}$ is an invadable repeller (fig. 5c), while for moderately strong trade-offs, it is strongly attracting and invadable and therefore an evolutionary branching point (fig. 5d). These two parameter regions are separated by a narrow region in which the singular point $\theta^*_{e,h}$ is weakly attracting. Given that in this quadrant the one-dimensional singular point θ^*_h is always an uninvadable attractor (see fig. 4d), one might expect that the properties of the one-dimensional singular point θ^*_e carry over to the case of joint trait evolution. However, a comparison of the pattern in the upper left quadrant in figure 5a with the corresponding quadrant in figure 4c shows that the parameter region for evolutionary branching becomes smaller under joint trait evolution.

Weak trade-off for e and weak trade-off for h (upper right quadrant in fig. 5a). In this parameter region, four different outcomes are possible. If both z_e and z_h are just slightly larger than zero, then $\theta^*_{e,h}$ is an evolutionary repeller (black region in the upper right quadrant of fig. 5a and fig. 5g). If z_e and z_h are slightly increased, then $\theta^*_{e,h}$ is strongly attracting and invadable and therefore an evolutionary branching point (orange region in the top right quadrant of fig. 5a and fig. 5e). These two regions are separated by a narrow band in which $\theta^*_{e,h}$ is weakly attracting (yellow region in the top right quadrant of fig. 5a). Finally, if both trade-offs are very weak, then $\theta^*_{e,h}$ is an uninvadable attractor and therefore an end point of evolution (green region in the top right quadrant of fig. 5a and fig. 5f). In this quadrant, both traits are uninvadable attractors when evolving separately. Thus, the results for joint trait evolution can clearly not be predicted from the analysis of the separately evolving traits. Note in particular that, unlike as in figure 4c and 4d, linear trade-offs no longer delimit different evolutionary outcomes.

To better understand why the evolutionary dynamics of jointly evolving traits can generally not be predicted from the evolutionary dynamics of the separately evolving traits, we consider three different mutant consumer individuals appearing in a resident population with the singular strategy $\theta^*_{e,h} = (0.5, 0.5)$. The first individual is specialized for resource 1 in terms of its feeding efficiencies ($\theta^m_e < 0.5$) but a generalist in terms of its handling times ($\theta^m_h = 0.5$). This mutation leads to an increased consumption rate of resource 1 at the cost of a decreased consumption rate of resource 2. This can be seen from equations (1a) and (1b), which are monotonically increasing functions of e_1 and e_2, respectively. The second individual is specialized in terms of its handling times for resource 1 ($\theta^m_h < 0.5$) but is a generalist in terms of its feeding efficiencies ($\theta^m_e = 0.5$). This mutation affects the time available
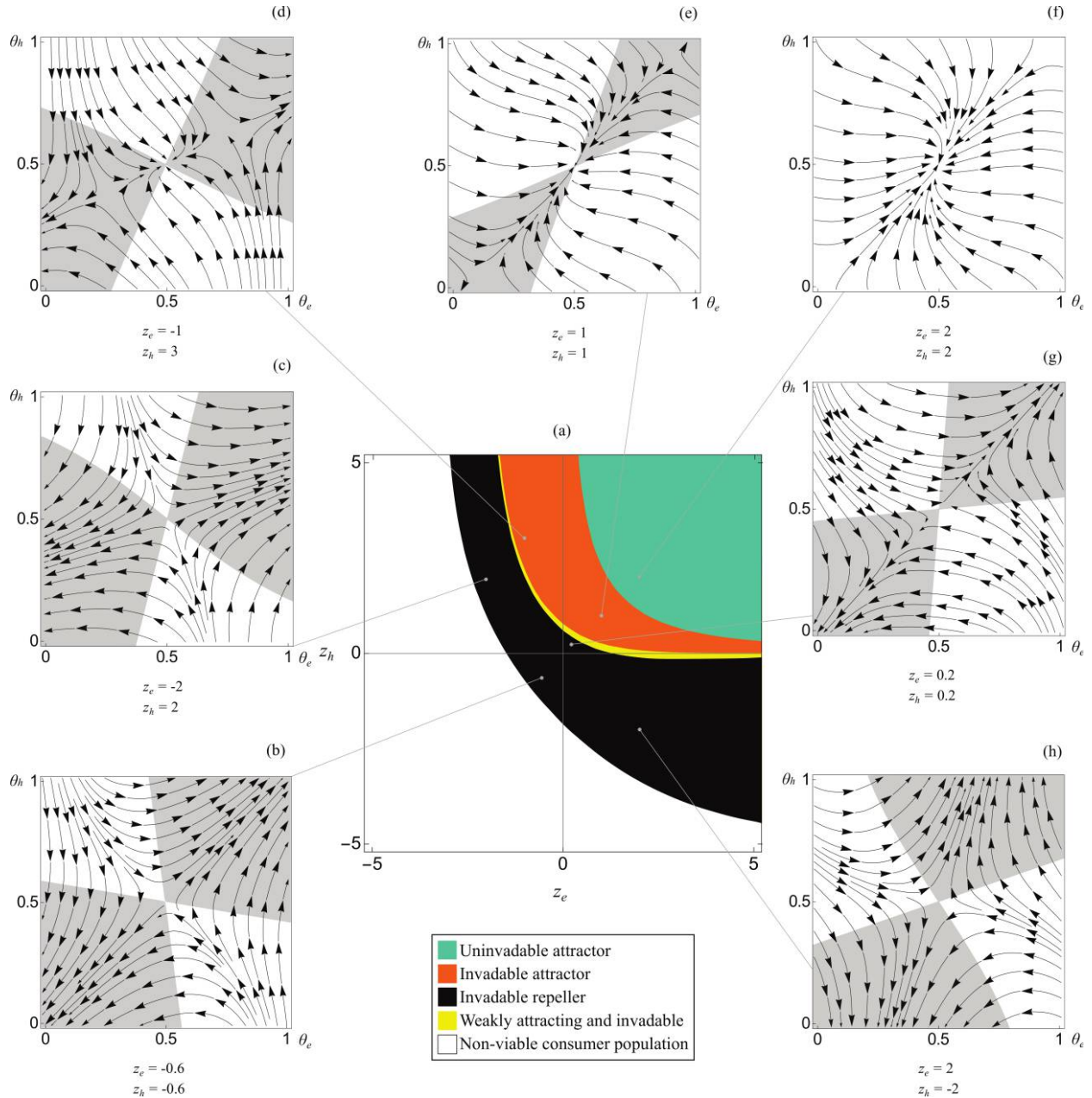
Figure 5: Joint evolutionary dynamics of feeding efficiency *e* and handling time *h*. *a*, Bifurcation diagram delimiting different evolutionary outcomes based on the trade-off curvature parameters z_e (*X*-axis) and z_h (*Y*-axis). The white region delimits trade-off combinations that result in nonviable consumer populations. Colors indicate the evolutionary behavior of the singular point $\theta^*_{e,h} = (0.5, 0.5)$: black, invadable repeller; yellow, invadable and weakly attracting (i.e., evolutionary branching point for suitable mutational variance-covariance matrices M); orange, invadable and strongly attracting (i.e., branching point); and green, uninvadable and attracting. *b–h*, Phase-plane diagrams of the joint evolutionary dynamics of feeding efficiency θ_e (*X*-axis) and handling time θ_h (*Y*-axis) for specific combinations of z_e and z_h. See figure 2 for a detailed introduction to these panels. Black arrows give evolutionary trajectories in trait space, and gray shading gives the sets of mutants able to invade the resident population with the singular strategy. Other parameters: $K_1 = 2.5 = K_2$, $\alpha_1 = 1 = \alpha_2$, $d = 0.9$.

for searching resources, which is inversely proportional to the denominator on the right-hand side of equation (4), and this affects the consumption of the two resources

equally. The third individual carries both changes of the two previous individuals ($\theta^m_e < 0.5$ and $\theta^m_h < 0.5$). This individual has an increased consumption of resource 1 and

simultaneously needs less time to process each item of this resource—the potential benefit of the first change is amplified by the second change. Thus, the joint effect of these two changes on fitness is not simply the sum of the effects of each change but is increased by an extra amount due to the positive interaction of the two changes. We say that the two traits show "positive epistatic interactions" on fitness. The positive epistatic interaction between e and h explains why the singular point $\theta_{e,h}^*$ can be invadable by mutants carrying changes in both traits even if the traits are uninvadable when evolving separately (e.g., fig. 5e, 5g).

Mathematically, this positive interaction manifests itself as follows. When e and h evolve one by one, invadability and attractivity are each determined by a single scalar quantity (see app. B). These scalars are the diagonal entries in the two-dimensional Hessian H (eq. [7]) and Jacobian J (eq. [8]), respectively. The eigenvalues of these matrices determine the invadability and attractivity of the two-dimensional singular point $\theta_{e,h}^*$, and, importantly, these eigenvalues also depend on the off-diagonal entries of H and J. For the Hessian matrix H, the off-diagonal entry

$$h_{e,h} = \frac{\partial^2 w(\boldsymbol{\theta}^m, \boldsymbol{\theta}^r)}{\partial \theta_e^m \partial \theta_h^m} \bigg|_{\boldsymbol{\theta}^m = \boldsymbol{\theta}^r = \boldsymbol{\theta}^*}$$

describes how the change in invasion fitness due to an increase in one trait value is altered by an increase in the other trait value. If this mixed derivative is positive, then the fitness of a mutant that carries changes in both traits exceeds the fitness that can be expected from the sum of the separate effects (cf. app. C, eq. [C2]). For our model we prove in appendix C, section C.1, that this mixed derivative is, in line with intuition, indeed always positive.

A consequence of the positive epistatic interactions is that the eigenvector corresponding to the dominant eigenvalue of H points to a direction in which the two trait values θ_e and θ_h increase. This can be seen in figure 5b–5h, in which the gray cones that correspond to mutants able to invade the singular strategy mostly cover the areas in which both trait values confer adaptations for the same resource. Conversely, most mutants that are specialized for one resource in terms of feeding efficiency and for the other resource in terms of handling time ($\theta_e > 0.5$ and $\theta_h < 0.5$ or $\theta_e < 0.5$ and $\theta_h > 0.5$) cannot invade, as these changes show negative epistatic interactions.

Whether or not the singular point $\theta_{e,h}^*$ is an attractor of the evolutionary dynamics is also affected by the off-diagonal entries of the Hessian since the off-diagonal entries of the Jacobian matrix J are given by $j_{e,h} = q_{e,h} + h_{e,h}$ (see eq. [8]). As a consequence, positive epistatic interactions between the two traits that favor invadability of the singular point $\theta_{e,h}^*$ make it also less likely that it is an attractor. Specifically, a singular point that is attracting in

both traits when these are evolving in isolation can be repelling under joint trait evolution in directions in which both θ_e and θ_h have values corresponding to specialization for the same resource. This is the case in the small black region in the upper right quadrant in figure 5a, as illustrated in figure 5g. We note that attractivity is also affected by the off-diagonal entries of the Q matrix, whose entries contain the mixed derivatives with respect to both mutant and resident traits (eq. [9]; app. C, eq. [C7]).

We conclude with two observations. First, when comparing the sequence of panels b, g, e, and f in figure 5, which show the evolutionary dynamics for increasingly weaker trade-offs, we see that the gray cones indicating the set of mutants that are able to invade the singular strategy become more narrow. Thus, with weaker trade-offs mutants have to be increasingly specialized to the same degree for invasion to be possible. Second, figure 5d and figure 5e show the joint evolutionary dynamics for combinations of trade-off curvatures for which the evolutionary branching point at $\theta_{e,h}^* = (0.5, 0.5)$ is accompanied by two further singular points that are both invadable and repelling. The evolutionary dynamics will then approach the branching point only when the initial population is not specialized in both traits for the same resource. This finding is a direct consequence of the fact that in the case when feeding efficiency evolves in isolation, the branching point at $\theta_e^* = 0.5$ is accompanied by two repelling singular strategies (fig. 4a).

Joint Evolution of Feeding Efficiency and Conversion Efficiency. Joint evolution of feeding efficiency e and conversion efficiency $\boldsymbol{\alpha}$ behaves qualitatively identical to joint evolution of feeding efficiency and handling time (see fig. E1a). This is to be expected, since qualitatively the evolutionary dynamics of conversion efficiency by itself is identical to that of handling time by itself.

Joint Evolution of Conversion Efficiency and Handling Time. Joint evolution of conversion efficiency $\boldsymbol{\alpha}$ and handling time h behaves very differently. Under the symmetry assumption $r_1 = r_2$, $K_1 = K_2$, and $e_1 = e_2$, the generalist strategy $\theta_{\alpha,h}^* = (\theta_\alpha^*, \theta_h^*) = (0.5, 0.5)$ is a unique singular point. Figure E1b shows its properties as a function of the curvature parameters z_a and z_h. If both trade-offs are weak, then the singular point $\theta_{\alpha,h}^*$ is an uninvadable attractor, and if one or both of the trade-offs is strong, then it is an invadable repeller. This is indeed what one would predict based on the analysis of the separately evolving traits (fig. 4b).

The reason for this simple result is that epistatic interactions on fitness between conversion efficiency $\boldsymbol{\alpha}$ and handling time h are absent. This is evident from the fact that

the Hessian matrix is a diagonal matrix (app. C, eq. [C12]). As explained in the section "Evolution of the Three Traits Separately," neither a mutation affecting handling time nor a mutation affecting conversion efficiency changes the uptake of one resource relative to the other. Rather, the first mutation changes the overall time available for searching for resources (which is proportional to 1 divided by the denominator of the first term on the right-hand side of eq. [4]), and this affects the uptake of the two resources equally. Similarly, the second mutation affects the growth rate of the consumer population, and this affects the resource dynamics in an indirect and equal manner. Combining the two changes does not change fitness beyond the separate effects of each change.

Furthermore, for this model the Q matrix is a null matrix resulting in J = H (app. C, sec. C.2). Thus, the singular point is an attractor if it is uninvadable and a repeller if it is invadable, implying that evolutionary branching is impossible. This also follows from the fact that for symmetric feeding efficiencies the two resource equilibrium densities $\hat{R}_1$ and $\hat{R}_2$ are equal to each other regardless of the degree of specialization of the resident population in terms of h and α (app. C, eq. [C10]). One can then prove that selection acts to minimize the resource equilibrium densities (Metz et al. 2008). These results are confirmed numerically for asymmetric parameters in figure E4*d*.

Joint Evolution of Three Traits. Under the symmetry assumption $r_1 = r_2$ and $K_1 = K_2$, the three-dimensional strategy $\boldsymbol{\theta}^*_{e,h,\alpha} = (\theta^*_e, \theta^*_h, \theta^*_\alpha) = (0.5, 0.5, 0.5)$ is a singular point. Figure 6 shows the properties of this singular point as a function of the curvature parameters z_e, z_h, and z_α. The cube shown in figure 6 can be divided into eight octants, depending on whether all three trade-offs are strong, only two of them are strong, only one of them is strong, or all are weak. For strong trade-offs in h or α, the singular point $\boldsymbol{\theta}^*_{e,h,\alpha}$ is an evolutionary repeller and evolution leads, depending on initial conditions, to a single phenotype that is specialized in all three traits for either resource 1 or resource 2. This accounts for six of the eight octants and corresponds to the bottom right quadrant in figure 5*a*.

When a strong trade-off in e is combined with weak trade-offs in both h and α (upper right back octant in fig. 6), two different scenarios are possible. The singular point $\boldsymbol{\theta}^*_{e,h,\alpha}$ is an evolutionary repeller for very strong trade-offs in e and turns into an evolutionary branching point for moderately strong trade-offs in e. This octant is the analogue to the top left quadrant in figure 5*a*.

When all three trade-offs are weak (upper right front octant in fig. 6), three outcomes are possible. First, if z_e, z_h, and z_α are just slightly larger than zero, then $\boldsymbol{\theta}^*_{e,h,\alpha}$ is an evolutionary repeller. Second, if z_e, z_h, and z_α are increased, then $\boldsymbol{\theta}^*_{e,h,\alpha}$ turns into an evolutionary branching point. Finally, if
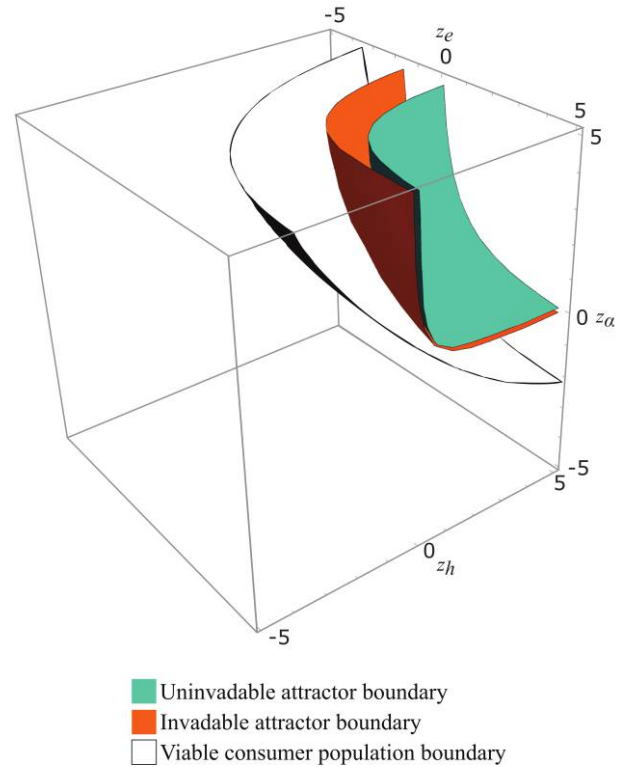

Figure 6: Bifurcation diagram delimiting different outcomes of the joint evolutionary dynamics of feeding efficiency e, handling time h, and conversion efficiency α based on the trade-off curvature parameters z_h (X-axis), z_α (Y-axis), and z_e (Z-axis). The white surface separates trade-off combinations that result in nonviable (*left*) and viable (*right*) consumer populations. Colored surfaces separate regions with different evolutionary behavior at the singular point $\boldsymbol{\theta}^*_{e,h,\alpha} = (0.5, 0.5, 0.5)$: orange, invadable repeller (*left*) and invadable attractor (i.e., branching point; *right*); green, invadable attractor (*left*) and uninvadable attractor (*right*). Between the orange and green surface the singular point is an attractor of the evolutionary dynamics independent of the mutational variance-covariance matrix M. Analogous to figure 5*a*, there exists a thin layer of parameter combinations below the orange surface in which the singular point is an attractor of the evolutionary dynamics only for suitable mutational variance-covariance matrices M. This additional surface is omitted for visual clarity. Other parameters: $K_1 = 2.5 = K_2, d = 0.9$.

all three trade-offs are very weak, then $\boldsymbol{\theta}^*_{e,h,\alpha}$ is an uninvadable attractor and an end point of evolution. This octant is the analogue to the top right quadrant in figure 5*a*.

In summary, the results for the joint evolution of three traits are very similar to those for the joint evolution of only e and h. Indeed, figure 5*a* can be thought of as the top surface of the cube in figure 6 (where $z_\alpha = 5$, resulting in approximately $\alpha_1 = 1 = \alpha_2$, as in fig. 5*a*). However, figure E5 shows that allowing α to evolve introduces subtle differences. In particular, in the top surface of figure 6 both the boundary between repelling and attracting and that

between invadable and uninvadable singular points is shifted toward weaker trade-offs. Thus, it is, for instance, possible to choose trade-off curvature parameters z_e and z_h such that $\theta^*_{e,h}$ is an evolutionary branching point that turns into an evolutionary repeller if α can evolve as well. Figure E6 discusses further differences that arise from increasing the number of jointly evolving traits.

We note that also in the case of three jointly evolving traits, combinations of trade-off curvatures exist for which the singular point $\theta^*_{e,h,\alpha}$ is an attractor of the evolutionary dynamics only for suitable mutational variance-covariance matrices M—that is, it is weakly attracting. Analogous to the case of joint evolution of e and h, this parameter region is a thin layer separating the region where the singular point is an evolutionary branching point from the region where it is a repeller. For three jointly evolving traits, this region is very thin and therefore omitted from figure 6 for clarity.

Discussion

Consumers generally experience trade-offs in their ability to find, handle, and digest different resources. This poses the question, under which conditions should we expect the evolution of specialist consumers that thrive on a small set of resources at the cost of being unable to utilize others or generalist consumers that can utilize a large set of resources reasonably well (Levins 1968; Futuyma and Moreno 1988; Wilson and Yoshimura 1994; Smith and Skúlason 1996; Kassen 2002; Forister et al. 2011)? More recent research has focused on identifying conditions under which specialists for different resources can emerge within a population due to negative frequency-dependent disruptive selection at so-called evolutionary branching points (e.g., Ma and Levin 2006; Rueffler et al. 2006b; Zu et al. 2011a).

Here, we study the joint evolution of up to three foraging-related traits (feeding efficiency, handling time, and conversion efficiency) in a consumer species, under the assumption that each of these traits is subject to a trade-off with respect to two resources. We focus on understanding how the conditions for evolutionary diversification at evolutionary branching points are altered when increasing the number of jointly evolving traits from one to two to three. We find that joint evolution can drastically alter the evolutionary dynamics by affecting the conditions under which the generalist strategy is an attractor of the evolutionary dynamics and invadable by nearby mutants. For singly evolving traits, linear trade-offs are the boundary between invadable and uninvadable singular points, and evolutionary branching is possible only for moderately strong trade-offs in feeding efficiency e (fig. 4). Under joint trait evolution, the conditions for the different evolutionary outcomes change whenever feeding efficiency is among the evolving traits. Importantly, the altered evolutionary

dynamics cannot be predicted from the single-trait analyses (figs. 5, 6, E5, E6). This is due to positive epistatic interactions on fitness between feeding efficiency and the other traits. Increasing the feeding efficiency for one resource increases the consumption rate of that resource. The resulting fitness benefit increases in a more than additive manner when combined with improvements in handling time or conversion efficiency for the same resource. Mathematically, positive epistatic effects are manifested as positive off-diagonal entries in the Hessian matrix of invasion fitness. A consequence of these epistatic interactions is that multidimensional singular points are more prone to be evolutionarily repelling and invadable in directions in which specialization occurs for the same resource in more than one trait. As a result, the range of trade-off curvatures for which evolutionary branching is possible is shifted toward weaker trade-offs. Interestingly, epistatic interactions are not present between handling time and conversion efficiency. The reason is that, everything else being equal, increasing the conversion efficiency or decreasing the handling time for one resource does not increase the consumption of that resource relative to the other. Rather, changes in these traits affect the consumption and equilibrium abundance of the two resources equally. As a consequence, the joint evolution of these two traits holds no surprises compared with the single-trait analyses (fig. E1b).

The three traits—handling time, conversion, and feeding efficiency—affect the foraging process at different steps, and we based our study on the assumption that different organs within an organism determine these characters. For instance, the probability of detecting prey items depends on sensory traits, while handling time and conversion efficiency depend on the feeding apparatus and the digestive system, respectively. This motivates our assumption that trade-offs exist within the same trait with respect to different resources (e.g., between the feeding efficiencies e_1 and e_2) but not between the different traits. In other words, a trait such as feeding efficiency does not trade off with conversion efficiency. There surely exist examples where this assumption is not valid, and we do not venture making predictions for such cases based on the present analysis.

In our analysis, it is assumed that mutations affect several traits, such as feeding efficiency and handling time, simultaneously. Specifically, the evolutionary dynamics described by equation (6) is based on the assumption that the distribution of mutations is governed by a symmetric variance-covariance matrix M whose off-diagonal entries describe mutational correlations. It has indeed been suggested that epistatic fitness interactions can result in the evolution of trait correlations through developmental coupling (for a review, see Armbruster et al. 2014). Importantly, for the largest part, our results are qualitatively independent of such correlations. While mutational correlations

can have a strong effect on the speed of population divergence (fig. D3), they alter neither the nature of a singular point nor the evolutionary end point. This is true as long as such correlations are not so extreme to effectively couple different traits. Having said this, we do find small regions in the bifurcation diagrams shown in figures 5*a* and E3, in which the generalist strategy is an evolutionary attractor for some variance-covariance matrices but not for others (see fig. E2). Such a dependence of evolutionary branching on the mutational process has also been found by Ravigné et al. (2009) and Débarre et al. (2014), and is not possible with only a single evolving trait.

Figure D4 shows additional simulations that are based on the assumption that feeding efficiency and handling time are coded by different genes such that each mutation affects only one of the traits at a time. The absence of pleiotropic mutations again only alters the speed of evolutionary diversification but—if population size is not too small—not the final outcome. Our simulations are furthermore based on the simplifying assumption of clonal reproduction. In sexual organisms, the positive linkage between genes that confer specialization for the same resource will be reduced by recombination, which much complicates the evolutionary dynamics after evolutionary branching (see Svardal et al. 2015). Interestingly, Mullon et al. (2018) show, in a study of a haploid sexual population undergoing evolutionary branching in two jointly evolving traits, that if the rate of recombination is itself subject to mutations, it evolves to ever lower values and thereby strengthens the linkage between traits with positive epistatic interactions.

Doebeli and Ispolatov (2010) proposed that increasing the number of jointly evolving traits generally increases the potential for evolutionary diversification in the sense that the proportion of parameter space resulting in evolutionary branching increases. This proposition was supported in two follow-up studies (Débarre et al. 2014; Svardal et al. 2014) but is at odds with several other studies (Bolnick and Doebeli 2003; Ackermann and Doebeli 2004; Van Dooren et al. 2004; Leimar 2009; Svardal et al. 2011). Does evolutionary diversification become more likely in our model as we increase the number of jointly evolving traits? For the traits considered in this study, table 1 gives the proportion of combinations of trade-off curvatures resulting in an uninvadable attractor, an evolutionary branching point, or an evolutionary repeller, depending on whether one, two, or three traits evolve. These proportions are calculated as the relative volume of the parameter space in figures 6 and E6 that corresponds to the different evolutionary outcomes, conditional on the consumer population being viable. According to these results, evolutionary branching becomes more likely when handling time is allowed to evolve jointly with feeding efficiency. However, if all three traits evolve jointly, then the likelihood for

Table 1: Likelihood (%) for different singular points as a function of the set of jointly evolving traits

	e	*e + h*	*e + h + α*
Uninvadable attractor	83	55	22
Branching point	8.2	14.6	8.6
Invadable repeller	8.8	30.4	69.4

Note: Percentages are calculated as the relative volume in figures 6 and E6 resulting in the different evolutionary properties, conditional on the consumer population being viable. Note that the size of the parameter space resulting in weakly attracting singular points, which is very small, is not reported separately but incorporated into that of invadable repellers.

evolutionary branching drops and is just very slightly increased compared with that when feeding efficiency evolves on its own. Thus, the results for our model show that, contrary to Doebeli and Ispolatov (2010), increasing the number of jointly evolving traits need not make evolutionary branching an ever more likely outcome of evolution.

Instead, the results in table 1 show two other trends. First, the likelihood that the generalist singular point is an evolutionary repeller, resulting in the evolution of a single consumer specialized for one of the resources, strongly increases with an increasing number of jointly evolving traits. This prompts a related question. Genetic polymorphism can emerge not only through gradual evolutionary change at an evolutionary branching point but also through immigration of consumers specialized for one resource into a population of consumers specialized for the other resource, and one might then wonder whether such an assembled community can also persist at an evolutionary timescale (Edwards et al. 2018). By this we mean that the two specialists do not undergo convergent evolution toward the generalist phenotype or, similarly, cannot be invaded and replaced by the generalist phenotype. In one-dimensional trait spaces, invadability of a singular point and mutual invadability of the two specialists—that is, their ecological coexistence—together imply that this is the case (see fig. 5 in Metz et al. 1996). By analogy, we conjecture for our model of joint trait evolution that long-term coexistence of two specialists is possible not only when the singular point is an evolutionary branching point but also when it is an evolutionary repeller as long as the feeding efficiencies of the assembled specialists have evolved sufficiently large differences to guarantee their ecological coexistence. Since the combined proportion of the parameter regions in which the singular point is an evolutionary repeller or branching point increases strongly with an increasing number of jointly evolving traits, we suggest that the potential for long-term coexistence of two specialists indeed increases with an increasing number of jointly evolving traits. As a flip side of this observation, we note that the likelihood that the generalist strategy is an uninvadable

attractor rapidly decreases with an increasing number of jointly evolving traits. Thus, one can phrase the results from this perspective as well: in our model, joint trait evolution significantly decreases the likelihood of finding a single generalist consumer as the final outcome of the evolutionary dynamics.

The conclusions drawn in the previous two paragraphs are based on the tacit assumption that the volume of the set of trade-off curvature values resulting in a certain evolutionary outcome is proportional to finding this outcome in nature. This would be true if each combination of trade-off curvatures would have a similar probability to be realized in nature. However, there is no reason why this should be the case. The fact is that data on the shape of trade-off curves are notoriously hard to come by, but existing observational data based on intraspecific (Parsons and Robinson 2007) and interspecific (Benkman 1993; Schluter 1993; Parsons and Robinson 2007; Konuma et al. 2013) variation suggest that strong trade-offs might not be rare, a statement that has recently been supported in an experimental evolution study of viruses (Meyer et al. 2016). These authors interpret their findings as support for ecologically driven resource polymorphism and ecological speciation, respectively. This interpretation surely goes back to the fitness set approach developed by Levins (1962) and is also in line with previous theoretical studies based on a single evolving trait in a consumer species feeding on two resources (Ma and Levin 2006; Rueffler et al. 2006b; Zu et al. 2011a). Our results suggest that great caution should be applied when making this inference, since under the more realistic assumption of joint trait evolution the range of trade-off curvatures that allows for evolutionary branching is shifted toward weaker trade-offs (fig. E5; also compare fig. 4c and 4d with fig. 5). What is clear in particular, is that—in the context of resource specialization—the simple dichotomy that weak trade-offs predict a resource generalist and strong trade-offs predict one or several resource specialists does generally not hold true.

Acknowledgments

Literature Cited

Abrams, P. A., H. Matsuda, and Y. Harada. 1993. Evolutionary unstable fitness maxima and stable fitness minima of continuous traits. Evolutionary Ecology 7:465–487.

Ackermann, M., and M. Doebeli. 2004. Evolution of niche width and adaptive diversification. Evolution 58:2599–2612.

Afik, D., and W. H. Karasov. 1995. The trade-off between digestion rate and efficiency in warblers and their ecological implications. Ecology 76:2247–2257.

Armbruster, W. S., C. Pélabon, G. H. Bolstad, and T. F. Hansen. 2014. Integrated phenotypes: understanding trait covariation in plants and animals. Philosophical Transactions of the Royal Society B 369:20130245.

Benkman, C. W. 1993. Adaptation to single resources and the evolution of crossbill (*Loxia*) diversity. Ecological Monographs 63: 305–325.

Bolnick, D. I. 2006. Multi-species outcomes in a common model of sympatric speciation. Journal of Theoretical Biology 241:734–744.

Bolnick, D. I., and M. Doebeli. 2003. Sexual dimorphism and adaptive speciation: two sides of the same ecological coin. Evolution 57:2433–2449.

Champagnat, N., R. Ferrière, and S. Méléard. 2006. Unifying evolutionary dynamics: from individual stochastic processes to macroscopic models. Theoretical Population Biology 69:297–321.

Claessen, D., and U. Dieckmann. 2002. Ontogenetic niche shifts and evolutionary branching in size-structured populations. Evolutionary Ecology Research 4:189–217.

Débarre, F., and S. Gandon. 2011. Evolution in heterogeneous environments: between soft and hard selection. American Naturalist 177:E84–E97.

Débarre, F., S. L. Nuismer, and M. Doebeli. 2014. Multidimensional (co)evolutionary stability. American Naturalist 184:158–171.

de Mazancourt, C., and U. Dieckmann. 2004. Trade-off geometries and frequency-dependent selection. American Naturalist 164: 765–778.

Dercole, F., and S. Rinaldi. 2008. Analysis of evolutionary processes: the adaptive dynamics approach and its applications. Princeton University Press, Princeton, NJ.

Dieckmann, U., and M. Doebeli. 1999. On the origin of species by sympatric speciation. Nature 400:354–357.

Dieckmann, U., M. Doebeli, J. A. J. Metz, and D. Tautz, eds. 2004. Adaptive speciation. Cambridge Studies in Adaptive Dynamics. Cambridge University Press, Cambridge.

Dieckmann, U., and R. Law. 1996. The dynamical theory of coevolution: a derivation from stochastic ecological processes. Journal of Mathematical Biology 34:579–612.

Doebeli, M. 2002. A model for the evolutionary dynamics of cross-feeding polymorphisms in microorganisms. Population Ecology 44:59–70.

———. 2011. Adaptive diversification. Monographs in Population Biology. Vol. 48. Princeton University Press, Princeton, NJ.

Doebeli, M., H. J. Blok, O. Leimar, and U. Dieckmann. 2007. Multimodal pattern formation in phenotype distributions of sexual populations. Proceedings of the Royal Society B 274:347–357.

Doebeli, M., and U. Dieckmann. 2000. Evolutionary branching and sympatric speciation caused by different types of ecological interactions. American Naturalist 156:S77–S101.

Doebeli, M., and I. Ispolatov. 2010. Complexity and diversity. Science 328:494–497.

Durinx, M., G. Meszéna, and J. A. J. Metz. 2008. Adapative dynamics for physiologically structured population models. Journal of Mathematical Biology 56:673–742.

Edwards, K. F., C. T. Kremer, E. T. Miller, M. M. Osmond, E. Litchman, and C. A. Klausmeier. 2018. Evolutionarily stable communities: a framework for understanding the role of trait evolution in the maintenance of diversity. Ecology Letters 21:1853–1868.

Egas, M., U. Dieckmann, and M. W. Sabelis. 2004. Evolution restricts the coexistence of specialists and generalists—the role of trade-off structure. American Naturalist 163:518–531.

Egas, M., M. W. Sabelis, and U. Dieckmann. 2005. Evolution of specialization and ecological character displacement of herbivores along a gradient of plant quality. Evolution 59:507–520.

Forister, M. L., L. A. Dyer, M. S. Singer, J. O. Stireman III, and J. T. Lill. 2011. Revisiting the evolution of ecological specialization, with emphasis on insect-plant interactions. Ecology 93:981–991.

Futuyma, D. J., and D. Moreno. 1988. The evolution of ecological specialization. Annual Reviews in Ecology and Systematics 19:207–233.

Geritz, S. A. H., and É. Kisdi. 2000. Adaptive dynamics in diploid, sexual populations and the evolution of reproductive isolation. Proceedings of the Royal Society B 267:1671–1678.

Geritz, S. A. H., É. Kisdi, G. Meszéna, and J. A. J. Metz. 1998. Evolutionarily singular strategies and the adaptive growth and branching of the evolutionary tree. Evolutionary Ecology 12:35–57.

Geritz, S. A. H., J. A. J. Metz, and C. Rueffler. 2016. Mutual invadability near evolutionarily singular strategies for multivariate traits, with special reference to the strongly convergence stable case. Journal of Mathematical Biology 72:1081–1099.

Heino, M., J. A. J. Metz, and V. Kaitala. 1998. The enigma of frequency-dependent selection. Trends in Ecology and Evolution 13:367–370.

Hendry, A. P., S. K. Huber, L. F. De León, A. Herrel, and J. Podos. 2009. Disruptive selection in a bimodal population of Darwin's finches. Proceedings of the Royal Society B 276:753–759.

Holling, C. S. 1959. Some characteristics of simple types of predation and parasitism. Canadian Entomologist 91:385–398.

Kassen, R. 2002. The experimental evolution of specialists, generalists, and the maintenance of diversity. Journal of Evolutionary Biology 15:173–190.

Kisdi, É., and S. A. H. Geritz. 1999. Adaptive dynamics in allele space: evolution of genetic polymorphism by small mutations in a heterogeneous environment. Evolution 53:993–1008.

Konuma, J., T. Sota, and S. Chiba. 2013. A maladaptive intermediate form: a strong trade-off revealed by hybrids between two forms of a snail-feeding beetle. Ecology 94:2638–2644.

Kopp, M., and J. Hermisson. 2008. Competitive speciation and costs of choosiness. Journal of Evolutionary Biology 21:1005–1023.

Lande, R. 1979. Quantitative genetic analysis of multivariate evolution, applied to brain : body size allometry. Evolution 33:402–416.

Leimar, O. 2005. The evolution of phenotypic polymorphism: randomized strategies versus evolutionary branching. American Naturalist 165:669–681.

———. 2009. Multidimensional convergence stability. Evolutionary Ecology Research 11:191–208.

Levene, H. 1953. Genetic equilibrium when more than one ecological niche is available. American Naturalist 87:331–333.

Levins, R. 1962. Theory of fitness in a heterogeneous environment. I. The fitness set and the adaptive function. American Naturalist 96:361–373.

———. 1968. Evolution in changing environments. Princeton University Press, Princeton, NJ.

Ma, J., and S. A. Levin. 2006. The evolution of resource adaptation: how generalist and specialist consumers evolve. Bulletin of Mathematical Biology 68:1111–1123.

Mackenzie, A. 1996. A trade-off for host plant utilization in the black ben aphid, *Aphis fabae*. Evolution 50:155–162.

Melin, A. D., L. M. Fedigan, C. Hiramatsu, C. L. Sendall, and S. Kawamura. 2007. Effects of colour vision phenotype on insect capture by a free-ranging population of white-faced capuchins, *Cebus capucinus*. Animal Behaviour 73:205–214.

Metz, J. A. J. 2008. Fitness. Pages 1599–1612 *in* S. Jørgensen and B. Fath, eds. Evolutionary ecology. Encyclopedia of Ecology. Vol. 2. Elsevier, Amsterdam.

Metz, J. A. J., S. A. H. Geritz, G. Meszéna, F. J. A. Jacobs, and J. S. Van Heerwaarden. 1996. Adaptive dynamics: a geometrical study of the consequences of nearly faithful reproduction. Pages 183–231 *in* S. van Strien and S. Verduyn Lunel, eds. Stochastic and spatial structures of dynamical systems, Proceedings of the Royal Dutch Academy of Science. North Holland, Dordrecht. http://pure.iiasa.ac.at/id/eprint/4497/.

Metz, J. A. J., S. D. Mylius, and O. Diekmann. 2008. When does evolution optimise? Evolutionary Ecology Research 10:629–654.

Metz, J. A. J., R. M. Nisbet, and S. A. H. Geritz. 1992. How should we define "fitness" for general ecological scenarios? Trends in Ecology and Evolution 7:198–202.

Meyer, J. R., D. T. Dobias, S. J. Medina, L. Servilio, A. Gupta, and R. E. Lenski. 2016. Ecological speciation of bacteriophage lambda in allopatry and sympatry. Science 354:1301–1304.

Mullon, C., L. Keller, and L. Lehmann. 2018. Social polymorphism is favoured by the co-evolution of dispersal with social behaviour. Nature Ecology and Evolution 2:132–140.

Nosil, P. 2012. Ecological speciation. Oxford Series in Ecology and Evolution. Oxford University Press, Oxford.

Nurmi, T., and K. Parvinen. 2013. Evolution of specialization under non-equilibrium population dynamics. Journal of Theoretical Biology 321:63–77.

Olsson, J., M. Quevedo, C. Colson, and R. Svanbäck. 2007. Gut length plasticity in perch: into the bowels of resource polymorphisms. Biological Journal of the Linnean Society 90:517–523.

Parsons, K. J., and B. W. Robinson. 2007. Foraging performance of diet-induced morphotypes in pumpkinseed sunfish (*Lepomis gibbosus*) favours resource polymorphism. Journal of Evolutionary Biology 20:673–684.

Pennings, P. S., M. Kopp, G. Meszéna, U. Dieckmann, and J. Hermisson. 2008. An analytically tractable model for competitive speciation. American Naturalist 171:E44–E71.

Pfennig, D. W., and K. S. Pfennig. 2012. Evolution's wedge—competition and the origin of diversity. University of California Press, Berkeley.

Rausher, M. D. 1984. Tradeoffs in performance on different hosts: evidence from within- and between-site variation in the beetle *Deloyala guttata*. Evolution 83:582–595.

Ravigné, V., U. Dieckmann, and I. Olivieri. 2009. Live where you thrive: joint evolution of habitat choice and local adaptation facilitates specialization and promotes diversity. American Naturalist 174:E141–E169.

Rettelbach, A., M. Kopp, U. Dieckmann, and J. Hermisson. 2013. Three modes of adaptive speciation in spatially structured populations. American Naturalist 182:E215–E234.

Ripa, J. 2009. When is sympatric speciation truly adaptive? an analysis of the joint evolution of resource utilization and assortative mating. Evolutionary Ecology 23:31–52.

Rosenzweig, M. L., and R. H. MacArthur. 1963. Graphical representation and stability conditions of predator-prey interactions. American Naturalist 97:209–223.

Rueffler, C., T. J. M. Van Dooren, O. Leimar, and P. A. Abrams. 2006*a*. Disruptive selection and then what? Trends in Ecology and Evolution 21:238–245.

Rueffler, C., T. J. M. Van Dooren, and J. A. J. Metz. 2006*b*. The evolution of resource specialization through frequency-dependent and frequency-independent mechanisms. American Naturalist 167:81–93.

Safi, K., and B. M. Siemers. 2010. Implications of sensory ecology for species coexistence: biased perception links predator diversity to prey size distribution. Evolutionary Ecology 24:703–713.

Schluter, D. 1993. Adaptive radiation in sticklebacks: size, shape, and habitat use efficiency. Ecology 74:699–709.

———. 1995. Adaptive radiation in sticklebacks: trade-offs in feeding performance and growth. Ecology 76:82–90.

———. 2000. The ecology of adaptive radiation. Oxford Series in Ecology and Evolution. Oxford University Press, Oxford.

Schneider, K. A., and R. Bürger. 2006. Does competitive divergence occur if assortative mating is costly? Journal of Evolutionary Biology 19:570–588.

Schreiber, S. J., and G. A. Tobiason. 2003. The evolution of resource use. Journal of Mathematical Biology 47:56–78.

Siemers, B. M., and S. M. Swift. 2006. Differences in sensory ecology contribute to resource partitioning in the bats *Myotis bechsteinii* and *Myotis nattereri* (chiroptera: Vespertilionidae). Behavioral Ecology and Sociobiology 59:373–380.

Smith, T. B., and S. Skúlason. 1996. Evolutionary significance of resource polymorphisms in fishes, amphibians, and birds. Annual Review of Ecology and Systematics 27:111–133.

Svardal, H., C. Rueffler, and M. Doebeli. 2014. Organismal complexity and the potential for evolutionary diversification. Evolution 3248–3259.

Svardal, H., C. Rueffler, and J. Hermisson. 2011. Comparing environmental and genetic variance as adaptive response to fluctuating selection. Evolution 65:2492–2513.

———. 2015. A general condition for adaptive genetic polymorphism in temporally and spatially heterogeneous environments. Theoretical Population Biology 99:76–97.

Van Dooren, T. J. M., I. Demon, and M. Durinx. 2004. Sexual dimorphism or evolutionary branching? Evolutionary Ecology Research 6:857–871.

van Doorn, G. S., P. Edelaar, and F. J. Weissing. 2009. On the origin of species by natural and sexual selection. Science 326:1704–1707.

Vasconcelos, P., and C. Rueffler. 2020. Data from: How does joint evolution of consumer traits affect resource specialization? American Naturalist, Dryad Digital Repository, https://doi.org/10.5061/dryad.ns1rn8pnf.

Wilson, D. S., and J. Yoshimura. 1994. On the coexistence of specialists and generalists. American Naturalist 144:692–707.

Wolfram Research. 2019. Mathematica. Ver. 12.0.

Zu, J., M. Mimura, and Y. Takeuchi. 2011*a*. Adaptive evolution of foraging-related traits in a predator-prey community. Journal of Theoretical Biology 268:14–29.

Zu, J., K. Wang, and M. Mimura. 2011*b*. Evolutionary branching and evolutionarily stable coexistence of predator species: critical function analysis. Mathematical Biosciences 231:210–224.

Symposium Editor: Maria R. Servedio
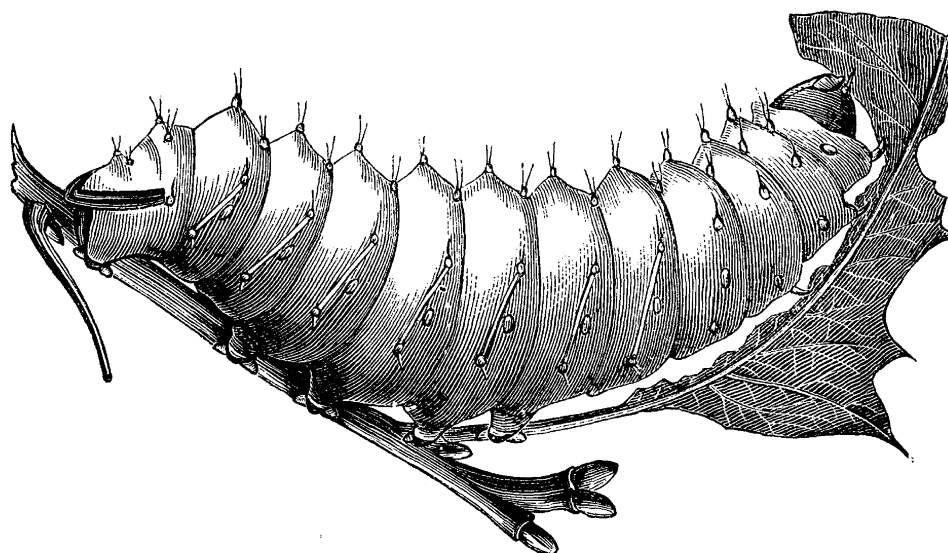
"Our country alone has eight or ten species of silk worms. Two of these, Callosamia Promethea and C. angulifera, feed on the lilac and wild cherry." From "The American Silk Worm" by L. Trouvelot (*The American Naturalist*, 1867, 1:30–38).